

¹ **Shaped to kill: The evolution of siphonophore tentilla**
² **for specialized prey capture in the open ocean**

³ Alejandro Damian-Serrano^{1,‡}, Steven H.D. Haddock², Casey W. Dunn¹

⁴ ¹ Yale University, Department of Ecology and Evolutionary Biology, 165 Prospect St.,
⁵ New Haven, CT 06520, USA

⁶ ² Monterey Bay Aquarium Research Institute, 7700 Sandholdt Rd., Moss Landing, CA
⁷ 95039, USA

⁸ [‡] Corresponding author: Alejandro Damian-Serrano, email: alejandro.damianserrano@
⁹ yale.edu

¹⁰ **Abstract**

¹¹ As predators evolve to feed on different prey taxa, their apparatus for prey capture can adapt
¹² into a variety of forms. The study of this evolutionary process is facilitated by a predator
¹³ clade with structures used exclusively for prey capture and with significant morphological
¹⁴ variation in these structures. Siphonophores, a clade of colonial cnidarians, satisfy these
¹⁵ criteria particularly well. Their tentilla (tentacle side branches) are the exclusive means of
¹⁶ prey capture for the large majority of species and have no other known function. Earlier
¹⁷ work has shown that extant siphonophore diets correlate with the different morphologies and
¹⁸ sizes of their tentilla and nematocysts. We hypothesize that evolutionary specialization on
¹⁹ different prey types has driven the phenotypic evolution of these characters. To test this
²⁰ hypothesis, we: (1) measured multiple morphological characters from siphonophore tentacle
²¹ specimens from 45 species, (2) mapped these data to a phylogenetic tree, and (3) analyzed
²² the evolutionary associations between morphological characters and prey type data from the
²³ literature. Our results show that siphonophore tentillum morphology has strong evolutionary
²⁴ associations with prey type, and suggest that shifts between prey type are linked to shifts in
²⁵ tentillum and nematocyst size and shape. We found that predatory specialists can evolve

26 into generalists, and that specialists on one prey type have directly evolved into specialists
27 on other prey types. When there are changes in trophic niche, both trait optima and trait
28 correlation patterns showed significant shifts. The evolutionary history of tentilla shows that
29 siphonophores are an example of ecological niche diversification via morphological innovation
30 and evolution. The extreme modularity of tentilla may have released siphonophores from the
31 evolutionary constraints of adaptation to ecologically specialized niches. This contributes to
32 understanding how morphological evolution has shaped present-day oceanic food webs.

33 **Keywords**

34 Siphonophores, tentilla, nematocysts, predation, specialization, character evolution

35 **Introduction**

36 Most animal predators use specific structures to capture and subdue prey. Raptors have
37 claws and beaks, snakes have fangs, wasps have stingers, and cnidarians have nematocyst-
38 laden tentacles. The functional morphology of these structures is critical to their ability
39 to successfully capture prey [1]. Long-term adaptive evolution in response to the defense
40 mechanisms of the prey (*e.g.*, avoidance, escape, protective barriers) leads to modifications
41 that can counter those defenses. The more specialized the diet of a predator is, the more
42 specialized its structures need to be to efficiently overcome the challenges posed by the
43 prey. Understanding the relationships between predatory and morphological specializations
44 is necessary to contextualize the phenotypic diversity of predators, quantify the importance
45 of ecological diversification in generating this diversity, and to understand the organismal
46 determinants of food web structure. However, for many clades of predators, there is scarce
47 knowledge on how these specializations evolved with each other. The primary questions
48 we set out to answer are: how do predator specialists and generalists evolve, and how does
49 predatory specialization shape morphological evolution?

50 Siphonophores (Cnidaria: Hydrozoa) are a clade of organisms bearing modular structures

51 that are exclusively used for prey capture: the tentilla (Fig. 1). The tentilla have great
52 morphological variation across species [2], which makes them an ideal system to study the
53 relationships between functional traits and prey specialization. Like a head of coral, a
54 siphonophore is a colony bearing many feeding polyps (Fig. 1). Each feeding polyp has a
55 single tentacle, which bears a series of side branches known as tentilla. Like other cnidarians,
56 siphonophores capture prey with nematocysts, harpoon-like stinging capsules borne within
57 specialized cells known as cnidocytes. Unlike the prey capture apparatus of most other
58 cnidarians, siphonophore tentacles carry their cnidocytes in extremely complex and organized
59 batteries [3] which are located in their tentilla. While nematocyst batteries and clusters in
60 other cnidarians are simple static scaffolds for cnidocytes, siphonophore tentilla have their
61 own reaction mechanism, triggered upon encounter with prey. When it fires, a tentillum
62 undergoes an extremely fast conformational change that wraps it around the prey, maximizing
63 the surface area of contact for nematocysts to fire on the prey [4]. In addition, some species
64 have elaborate fluorescent and bioluminescent lures on their tentilla to attract prey with
65 aggressive mimicry [5–7].

66 Siphonophores bear four major nematocyst types in their tentacles and tentilla (Fig. 1F)..
67 The largest type, heteronemes, have open-tip tubules characterized by bearing a distinctly
68 wider spiny shaft at the proximal end of the everted tubule. These are typically found flanking
69 the proximal end of the cnidoband. The most abundant type, haplonemes, have no distinct
70 shaft, but similarly to heteronemes, their tubules have open tips and can be found in the
71 cnidoband. Both heteronemes and haplonemes bear short spines along the tubule and can be
72 toxic and penetrate the surface of some prey types. In the terminal filament, siphonophores
73 bear two other types of nematocysts, characterized by their adhesive function, closed tip
74 tubules, and lack of spines on the tubule. These are the desmonemes (a type of adhesive
75 coiled-tubule spironeme), and rhopalonemes (a siphonophore-exclusive nematocyst type with
76 wide tubules).

77 Many siphonophore species inhabit the deep pelagic ocean, which spans from ~200m to the

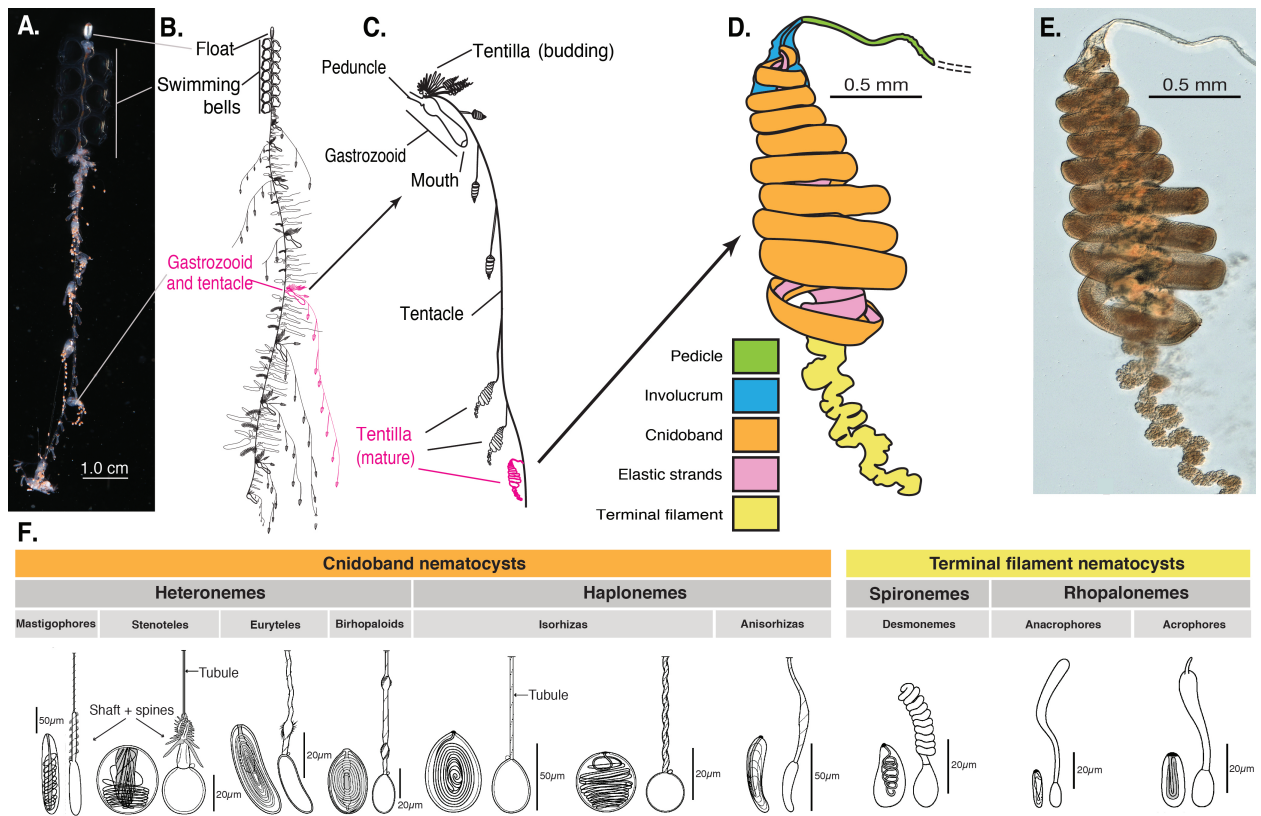


Figure 1: Siphonophore anatomy. A - *Nanomia* sp. siphonophore colony (photo by Catriona Munro). B, C - Illustration of a *Nanomia* colony, gastrozooid, and tentacle (by Freya Goetz). D - *Nanomia* sp. Tentillum illustration and main parts. E - Differential interference contrast micrograph of the tentillum illustrated in D. F - Nematocyst types (illustration reproduced with permission from Mapstone 2014), hypothesized homologies, and locations in the tentillum. Undischarged to the left, discharged to the right.

78 abyssal seafloor (~4000m). This habitat has fairly homogeneous physical conditions and stable
79 zooplankton abundances and composition [8]. With a relatively predictable prey availability,
80 ecological theory predicts that interspecific competition would inhibit the coexistence of
81 closely-related species unless evolution towards specialization reduces the breadth of each
82 species' niche [9–11]. If this prediction holds true, we would expect the prey capture apparatus
83 morphologies of siphonophores to diversify with the evolution of increasing specialization on
84 a variety of prey types in different siphonophore lineages.

85 Specialization has been thought to be an evolutionary ‘dead-end’, meaning that specialized
86 lineages are unlikely to evolve into generalists or to shift the resource for which they are
87 specialized [12–16]. However, recent studies have found that interspecific competition can
88 favor the evolution of resource generalism [17–19] and resource switching [20,21]. In addition
89 to studying relationships with morphology, we seek to identify what evolutionary transitions
90 in trophic niche breadth are prevalent in open-ocean tactile predators. To do so, we examine
91 three alternative scenarios of siphonophore trophic specialization: (1) predatory specialists
92 evolved from generalist ancestors; (2) predatory specialists evolved from specialist ancestors
93 which targeted different resources, switching their primary prey type; and (3) predatory
94 generalists evolved from specialist ancestors. These scenarios are non-exclusive, and each
95 could apply to different transitions along the siphonophore phylogeny.

96 The study of siphonophore tentilla and diets have been limited in the past due to the
97 inaccessibility of their oceanic habitat and the difficulties associated with the collection of
98 fragile siphonophores. Thus, the morphological diversity of tentilla has only been characterized
99 for a few taxa, and their evolutionary history remains largely unexplored. Contemporary
100 underwater sampling technology provides an unprecedented opportunity to explore the
101 trophic ecology [22] and functional morphology [23] of siphonophores. In addition, well-
102 supported phylogenies based on molecular data are now available for these organisms [24].
103 These advances allow for the examination of the evolutionary relationships between modern
104 siphonophore form, function, and ecology.

105 Our work builds upon previous pioneering studies that have explored the relationships
106 between tentilla and diet, and showed that siphonophores are a robust system for the study
107 of predatory specialization via morphological diversification. [25] and [26] showed clear
108 relationships between diet, tentillum, and nematocyst characters in co-occurring epipelagic
109 siphonophores for a small subset of extant epipelagic siphonophore species.

110 In this study, we characterize the morphological diversity of tentilla and their nematocysts
111 across a broad variety of shallow and deep-sea siphonophore species using modern imaging
112 technologies, we expand the phylogenetic tree of siphonophores by combining ribosomal gene
113 sequences from a broad range of taxa with a transcriptome-based backbone tree, and we
114 explore the evolutionary histories and correlations between diet, tentillum, and nematocyst
115 characters.

116 Results

117 *Novel phylogenetic relationships* – We built upon the published siphonophore transcriptome
118 phylogeny [24] to produce a tree with broader taxonomic representation using ribosomal
119 genes. The topology of our tree recapitulates the resolved nodes in [27] and [24]. Only 5
120 nodes (blue dots in Figure 2) in the unconstrained tree inference were incongruent with the
121 [24] transcriptome tree, and these were constrained to the [24] topology during estimation of
122 the constrained 18S+16S tree inference (Fig. 2). Moreover, with the inclusion of *Stephanomia*
123 *amphytridis* sequences, our tree reveals a novel phylogenetic relationship between the genus
124 *Erenna* and *Stephanomia*.

125 We used the clade nomenclature defined in [27] and [24], including Codonophora to
126 indicate the sister group to Cystonectae, Euphysonectae to indicate the sister group to
127 Calycophorae, Clade A and B to indicate the two main lineages within Euphysonectae. In
128 addition, we define two new clades within Codonophora (Fig. 2): Eucladophora as the
129 clade containing *Agalma elegans* and all taxa that are more closely related to it than to
130 *Apolemia lanosa*, and Tendiculophora as the clade containing *Agalma elegans* and all taxa

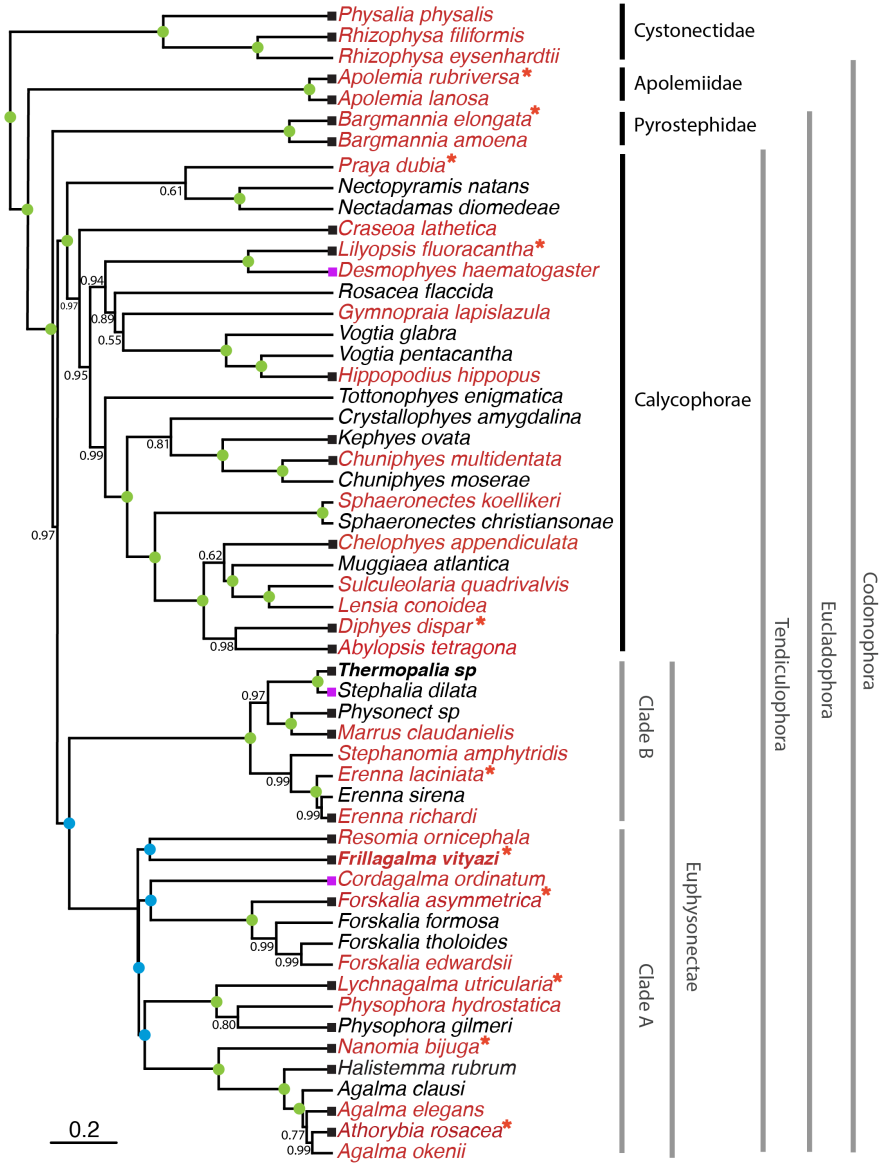


Figure 2: Bayesian time-tree built from 18S + 16S concatenated sequences. Branch lengths estimated using a relaxed molecular clock. Species names in red indicate replicated representation in the morphology data. Species marked with a red asterisk were recorded using high-speed video. Newly accessioned 16S data was used for species with names in bold. Nodes labeled with Bayesian posteriors (BP). Green circles indicate BP = 1. Blue circles indicate nodes constrained to be congruent with Munro *et al.* (2018). Tips with black squares indicate the species with transcriptomes used in Munro *et al.* (2018). Tips with grey squares indicate genus-level correspondence to taxa included in Munro *et al.* (2018). The main clades are labeled: in black for described taxonomic units, and in grey for operational phylogenetic designations.

¹³¹ more closely related to it than to *Bargmannia elongata*. Eucladophora is characterized by
¹³² bearing spatially differentiated tentilla with proximal heteronemes and a narrower terminal
¹³³ filament region. The etymology derives from the Greek *eu+kládos+phóros* for “true branch
¹³⁴ bearers”. Tendiculophora are characterized by bearing rhopalonemes and desmonemes in the
¹³⁵ terminal filament, having a pair of elastic strands, and developing proximally detachable
¹³⁶ cnidobands. The etymology of this clade is derived from the Latin *tendicula* for “snare or
¹³⁷ noose” and the Greek *phóros* for “carriers”.

¹³⁸ *Evolutionary associations between diet and tentillum morphology* – Reconstructions of
¹³⁹ feeding guilds do not recover ancestral diet generalism. None of the transitions in diet are
¹⁴⁰ consistent with scenario 1 (specialists evolving from generalists). Feeding guild specializations
¹⁴¹ have shifted from an alternative ancestral state at least five times, consistent with instances
¹⁴² supporting scenario 2 (specialists evolving to feed on a different resource). Copepod special-
¹⁴³ ization and fish specialization evolved twice, and ostracod specialization evolved at least once.
¹⁴⁴ We also recover multiple independent origins of generalism from specialist ancestors (Fig.
¹⁴⁵ 3). Large crustacean specialists evolve into generalists twice independently, consistent with
¹⁴⁶ instances of scenario 3 (generalists evolving from specialists). This finding is particularly
¹⁴⁷ compelling given in that it is the opposite of known biases in ancestral state reconstruction.
¹⁴⁸ [28] found that such methods tend to infer higher transition rates toward the more frequent
¹⁴⁹ state. In this case, that would lead to a bias for an increased rate of transition from generalists
¹⁵⁰ (the rarer state across the tips) to specialists (the more common state across the tips). We
¹⁵¹ observe the opposite, indicating strong evidence that these generalists are indeed a derived
¹⁵² state.

¹⁵³ To test whether measured morphological characters evolved in association with shifts in
¹⁵⁴ feeding ecology, we analyzed the evolutionary history of each character on the phylogeny,
¹⁵⁵ with the feeding guilds reconstructed on it as hypothetical selective regimes. We fitted
¹⁵⁶ and compared alternative evolutionary models for each continuous character. The models
¹⁵⁷ compared were the white noise (WN; non-phylogenetic model that assumes all values come

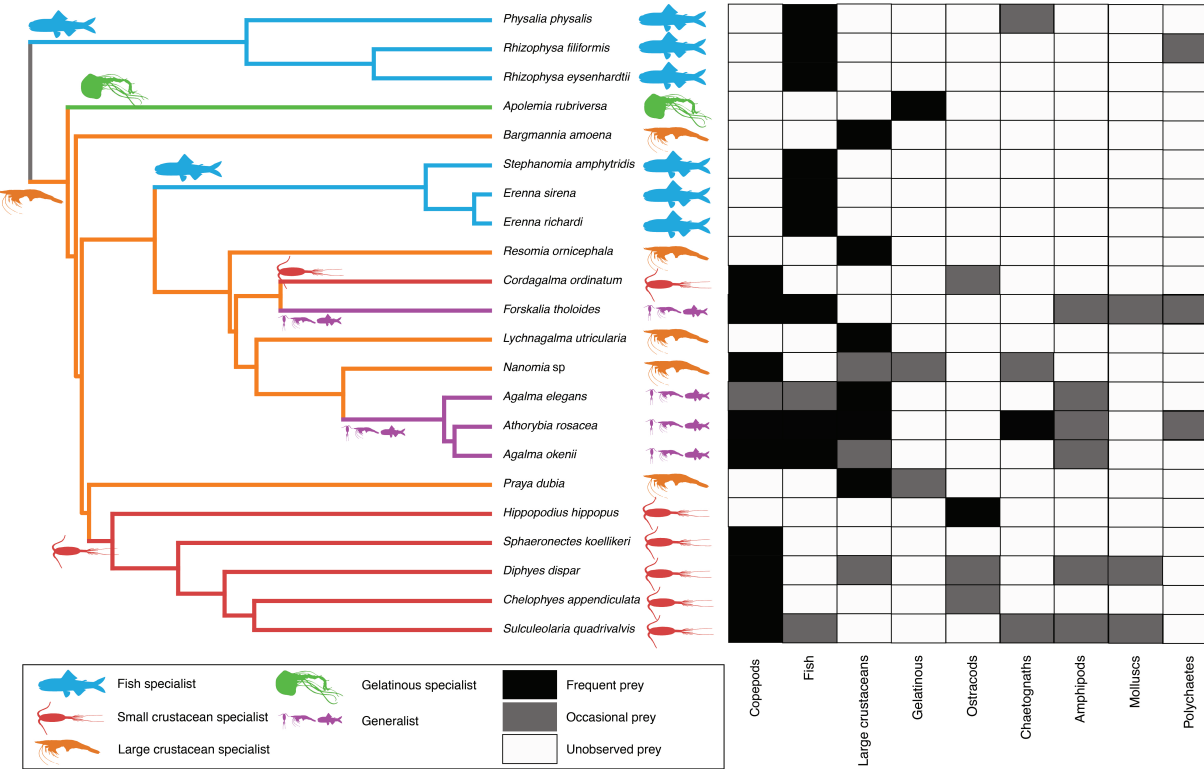


Figure 3: Left - Subset phylogeny showing the mapped feeding guild regimes that were used to inform the *OUwie* analyses. Right - Grid showing the prey items consumed from which the feeding guild categories were derived. Diet data were obtained from the literature review, available in the Dryad repository.

from a single normal distribution with no covariance structure among species), the Brownian Motion (BM) model of neutral divergent evolution [29], the Early Burst (EB) model of decreasing rate of evolutionary change [30], and the Ornstein-Uhlenbeck (OU) model of stabilizing selection around a fitted optimum state [31,32]. The model comparison shows that out of 30 characters, 10 show significantly stronger support for the diet-driven multi-optima multi-rate OU model (SM15). These characters include terminal filament nematocyst size and shape, involucrum length, elastic strand width, and heteroneme number. Most of these characters are found exclusively in Tendiculophora, thus this may reflect processes that could be unique to this subtree. Five characters including cnidoband length, cnidoband shape, and haploneme length show maximal support for a diet-driven single-optimum OU model. The remaining 15 characters support BM (or OU with marginal AICc difference with BM).

169 In order to investigate the associations between the evolutionary history of morphological
170 characters and specific prey types found in the diet, we used phylogenetic logistic regressions.
171 We found that several characters were significantly correlated with the gains and losses of
172 these prey types (Fig. 3, right). Shifts toward ostracod presence in diet correlated with
173 reductions in pedicle width and total haploneme volume. Shifts to copepod presence in
174 the diet were associated with reductions in haploneme width, cnidoband length and width,
175 total haploneme and heteroneme volumes, and tentacle and pedicle widths. Consistently,
176 transitions to decapod presence in the diet correlated with more coiled cnidobands (SM21).
177 Evolutionary shifts in these characters likely allowed the inclusion of these prey types in the
178 diet.

179 We also tested for correlations between shifts in prey selectivity and morphological
180 characters using phylogenetic linear models. We found that fish selectivity is associated
181 with increased number of heteronemes per tentillum, increased roundness of nematocysts
182 (desmonemes and haplonemes), larger heteronemes, reduced heteroneme/cnidoband length
183 ratios, smaller rhopalonemes, lower haploneme SA/V ratios, and larger the cnidoband, elastic
184 strand, pedicle and tentacle widths. Decapod-selective diets were associated with increasing
185 cnidoband size and coiledness, haploneme row number, elastic strand width, and heteroneme
186 number. Copepod-selective diets evolved in association with smaller heteroneme and total
187 nematocyst volumes, smaller cnidobands, rounder rhopalonemes, elongated heteronemes,
188 narrower haplonemes with higher SA/V ratios, and smaller heteronemes, tentacles, pedicles,
189 and elastic strands. Selectivity for ostracods was associated with reductions in size and
190 number of heteroneme nematocysts, reductions in cnidoband size, number of haploneme
191 rows, heteroneme numbers, and cnidoband coiledness. Heteroneme length and elongation
192 also correlated negatively with chaetognath selectivity (SM21). These results indicate that
193 not only diet but also differential feeding selectivity has evolved in correlation with changes
194 in the prey capture apparatus of siphonophores.

195 We tested some of the diet-morphology associations previously proposed in the literature

[25,26] for correlated evolution (Table 1). We found that most, such as heteroneme volume and copepod prey size, do show correlated evolution, consistent with these earlier hypotheses. The sole exception was the relationship between terminal filament nematocysts (rhopalonemes and desmonemes) and crustaceans in the diet. Analyses that do not take phylogeny into account do recover this correlation across the extant species studied, but it is not consistent with correlated evolution. The latter is likely a product of the larger species richness of crustacean-eating species with terminal filament nematocysts, rather than simultaneous evolutionary gains.

Table 1. Tests of correlated evolution between morphological characters and aspects of the diet found correlated in the literature.

Character	Aspect of diet	Test of evolutionary association	Relationship sign	P-value	Number of taxa	Association first report
Differentiated cnidobands	Hard bodied prey	Page's test	+	0.017	19	Purcell, 1984
Heteroneme volume	Copepod prey size	pGLS	+	0.002	8	Purcell, 1984
Terminal filament nematocysts	Crustacean diet	Page's test	Non-Significant	0.200	19	Purcell & Mills, 1988
Number of nematocyst types	Soft-bodied prey	Phylogenetic logistic regression	-	0.040	22	Purcell & Mills, 1988

Table 2. Discriminant analysis of principal components for the presence of specific prey types using the morphological data. Top quartile variable (character) contributions to the linear discriminants are ordered from highest to lowest. Logistic regressions and GLMs were fitted to predict prey type presence and selectivity respectively. The sign of the slope of each predictor is reported, marked with an asterisk if significant ($p\text{-value} < 0.05$), and highlighted grey if it differs between prey presence in diet and prey selectivity. Pseudo- R^2 (%) approximates the percent variance explained by the model.

Prey type	DAPC	GLM for prey type presence (22 taxa)		Best fitting GLM for prey type selectivity (Purcell, 1981) (7 taxa)	
		Discrimination (%)	Top quartile variable contributions	Sign	Pseudo-R ² (%)
Copepods	95.4	Total nematocyst volume	-	-*	
		Tentacle width	-	+	
		Haploneme elongation	-	+	
		Haploneme surface area/volume ratio	+	-	
		Haploneme row number	+	+	
		Cnidoband length	-	+	
		Cnidoband width	-	-	
		Cnidoband free length	+	+	
Fish	68.1	Total haploneme volume	-	+	
		Heteroneme volume	+	-	
		Total nematocyst volume	-	+	
		Total heteroneme volume	-	-	
		Cnidoband length	-	-	
		Cnidoband free length	+	+	
		Involucrum length	-	-	
		Pedicle width	+	+	
Large crustaceans	81.8	Involucrum length	++*	+	
		Total heteroneme volume	-	-	
		Elastic strand width	-	++*	
		Rhopaloneme length	+	+	
		Heteroneme volume	+	-	
		Haploneme elongation	-	+	
		Desmoneme length	-	-	
		Tentacle width	+	+	

215

216 *Evolution of the integrated tentillum morphology* – Phenotypic integration results in
 217 correlation patterns between morphological characters and their rates of evolution. To
 218 study these patterns, we fit a set of evolutionary variance-covariance matrices [33]. The
 219 quantitative characters we measured from tentilla and their nematocysts are highly correlated.
 220 The results indicate that the dimensionality (number of independent axes of variation) of
 221 tentillum morphology is low, that many traits are associated with size, but that nematocyst
 222 arrangement and shape are independent of it (SM4). The variance-covariance matrices
 223 (SM36-38) are congruent with the abundant positive correlations observed among simple
 224 measurement characters in SM3. This analysis more clearly reveals the diagonal blocks that
 225 constitute the evolutionary modules, such as the heteroneme block, the terminal filament
 226 nematocyst block, and the cnidoband-pedicle-tentacle block. These results were not sensitive
 227 to the transformation of inapplicable states and taxon sampling. These results indicate that
 228 siphonophore tentilla and nematocysts are phenotypically integrated and co-evolve within
 229 discrete evolutionary modules.

230 In order to test whether rate covariance matrices changed with evolutionary shifts in

231 feeding guild regimes, we compared the rate covariance terms between characters across
232 the subtrees occupied by the different feeding guild regimes (SM41). We found that half
233 (48%) of the character pairs presented significantly distinct correlation coefficients across
234 different regimes (SM39), indicating that the mode of phenotypic integration also shifts
235 with trophic niche. When contrasting the regime-specific rate correlation matrices to the
236 whole-tree matrix, we were able to identify the character dependencies that are unique to
237 each predatory niche (SM42). These results indicate that the evolutionary dependencies
238 in these integrated modules are changing across the phylogeny, and evolving together with
239 changes in prey type specializations.

240 We were able to identify specific character correlations that shifted with the evolution of
241 new diets. Under the majority of SIMMAP outcomes, large crustacean specialists are the
242 ancestral feeding regime, and all other feeding regimes evolve from this ancestral specialization.
243 Compared to the rate correlation matrix estimated over the whole tree, large crustacean
244 specialists present strong negative correlations between haploneme elongation and heteroneme
245 size, and between rhopaloneme elongation and tentillum size, as well as with involucrum
246 length. Within generalist clades (*Forskalia* and the *Agalma-Athorybia* clade), terminal
247 filament nematocyst (desmonemes and rhopalonemes) sizes became negatively correlated with
248 the sizes of most characters, meaning that as some tentilla became larger, their individual
249 terminal nematocysts became smaller, observed to the extreme in *Agalma*. In addition,
250 heteroneme and rhopaloneme elongation became positively correlated with cnidoband size.
251 When large crustacean specialists switched to small crustacean prey in *Cordagalma* and
252 calycophorans, haploneme size became inversely correlated with heteroneme elongation,
253 which in turn developed a strong positive relationship with tentillum size. In other words, as
254 tentilla get smaller in this group, heteronemes get shorter and haplonemes get larger. The
255 extremes of this gradient can be seen in *Cordagalma* and *Hippopodius*. With the evolution
256 of fish prey specialization in cystonects and within Clade B, haploneme elongation became
257 negatively correlated with heteroneme elongation (signal driven by Clade B, since cystonects

258 lack tentacular heteronemes), and the surface area to volume ratio of haploneme nematocysts
259 switched from a strong negative relationship with cnidoband size (found in every other
260 regime) to a positive correlation. Gelatinous specialization, albeit appearing only once in our
261 tree, also carries a unique signature in character rate correlation shifts, with an increase in
262 the strength of the correlation between heteroneme shape and shaft width, consistent with
263 the appearance of birrhopaloid nematocysts with swollen shafts that are likely effective at
264 anchoring gelatinous tissue (see reference to Narcomedusae nematocysts in [26]).

265 *Evolution of nematocyst shape* – The greatest evolutionary change in haploneme nemato-
266 cyst shape occurred in a single shift towards elongation in the stem of Tendiculophora, which
267 contains the majority of described siphonophore species other than Cystonects, *Apolemia*,
268 and Pyrostephidae. There is one secondary return to more oval, less elongated haplonemes in
269 *Erenna*, but it does not reach the sphericity present in Cystonectae or Pyrostephidae (Fig.
270 4). Heteroneme evolution presents a less discrete evolutionary history, where Tendiculophora
271 evolved more elongate heteronemes, but the difference between theirs and other siphonophores
272 is much smaller than the variation in shape within Tendiculophora, bearing no phylogenetic
273 signal. In this clade, the evolution of heteroneme shape has diverged in both directions, and
274 there is no correlation with haploneme shape (Fig. 4), which has remained fairly constant
275 (elongation between 1.5 and 2.5).

276 Discussion

277 *Evolution of siphonophore trophic niche* – Siphonophores are an abundant group of zooplankton
278 in oceanic ecosystems [34,35]. While little is known about siphonophore trophic ecology, what
279 is known indicates that they occupy a central position in midwater food webs [22], serving
280 as important trophic intermediaries between smaller zooplankton and higher trophic level
281 predators. Siphonophore species have been observed to feed on a variety of prey with very
282 different sizes, traits, and behaviors. Because there is a total absence of siphonophores in
283 the fossil record, how they became established as such ubiquitous and trophically diverse

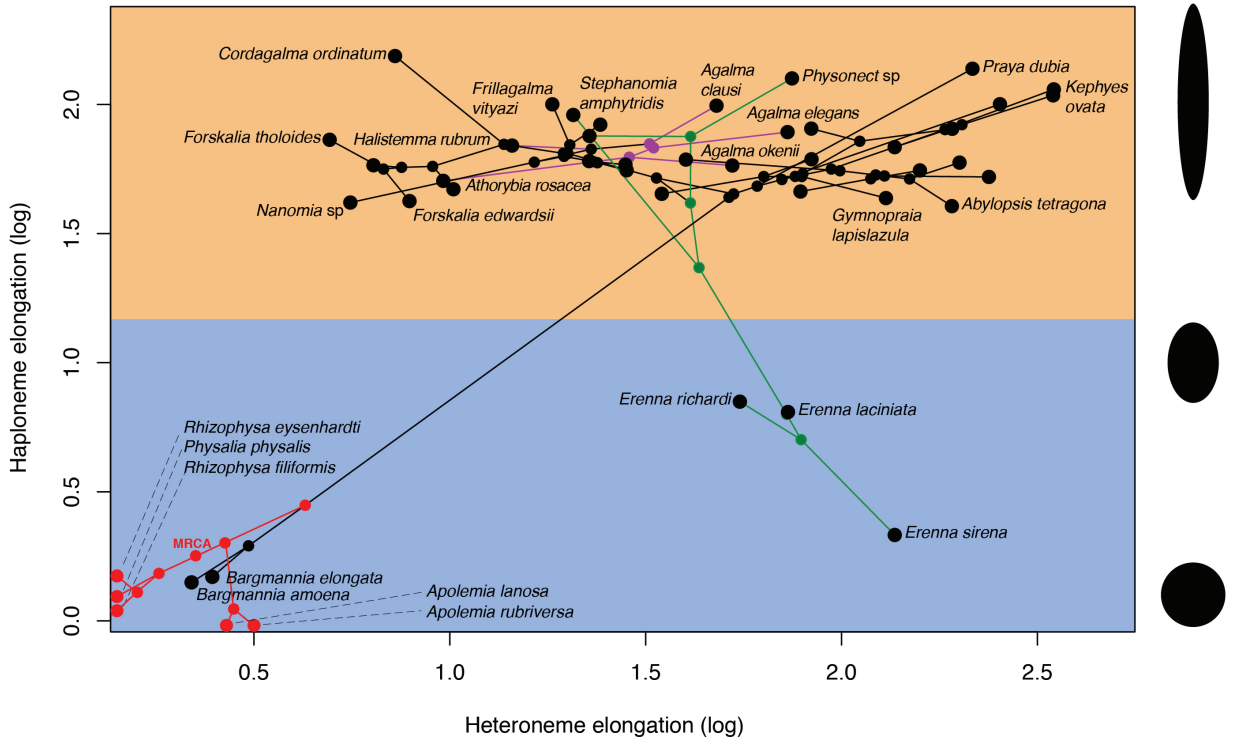


Figure 4: Phylomorphospace showing haploneme and heteroneme elongation (log scaled). Orange area delimits rod-shaped haplonemes, the blue area covers oval and round-shaped haplonemes. Smaller dots and lines represent phylogenetic relationships and ancestral states of internal nodes under BM. Species nodes in red were manually added to the plot. Cystonects have no tentacle heteronemes and are projected onto the haploneme axis. Apolemiids have no tentacle haplonemes and are projected onto the heteroneme axis. Colored branches and nodes correspond to BAMM regimes of accelerated haploneme shape (green) and heteroneme shape (violet) evolution.

²⁸⁴ predators in today's oceans remains an open question.

²⁸⁵ Several studies [12–16] have suggested that resource specialization is an irreversible dead-
²⁸⁶ end due to the constraints posed by extreme phenotypic specialization. Our results show
²⁸⁷ that this is not the case for siphonophores, where the prey type on which they specialize has
²⁸⁸ shifted at least 5 times. We find no support for any transitions from generalist to specialist
²⁸⁹ (scenario 1, as described in the Introduction). We do find support for at least 3 instances of
²⁹⁰ specialists switching from one prey type to another prey type, (scenario 2) and two switches
²⁹¹ from specialist to generalist (scenario 3).

²⁹² This is consistent with the findings of recent studies on phytophagous insects [19], where
²⁹³ the rate of evolution from generalists to specialists is comparable to the reverse, thus
²⁹⁴ specialization does not limit further evolution. Our results are also consistent with analyses
²⁹⁵ of lepidopterans [21], where specialized resource switching is the primary transition type
²⁹⁶ while niche breadth remains fairly constant. The evolutionary history of tentilla shows that
²⁹⁷ siphonophores are an example of trophic niche diversification via morphological innovation
²⁹⁸ and evolution, which allowed transitions between specialized trophic niches. In more familiar
²⁹⁹ predators, the prey capture apparatus is well integrated in the body (such as claws and
³⁰⁰ jaws), leading to trade-offs and whole body adaptations to feeding specialization. The
³⁰¹ extreme modularity of the siphonophore prey capture apparatus could release them from the
³⁰² constraints typically imposed by adaptation to ecological specialization. This evolutionary
³⁰³ mechanism is particularly important in a deep open ocean ecosystem, which is a relatively
³⁰⁴ homogeneous physical environment, where the primary niche heterogeneity available is the
³⁰⁵ potential interactions between organisms [8].

³⁰⁶ *Evolution of nematocyst shape* – The phylogenetic relationship of siphonophores to other
³⁰⁷ hydrozoans remains an unresolved question [24]. The most recent work on this front sets
³⁰⁸ them as the sister group to all other Hydrozoa [36]. Therefore, there is great uncertainty
³⁰⁹ around the ancestral plesiomorphies of the common ancestor of all siphonophores. This is
³¹⁰ especially true for those characters that present extreme differences between Cystonectae

and Codonophora (the earliest split in the siphonophore phylogeny). One such character is the shape of haploneme nematocysts. A remarkable feature of siphonophore haplonemes is that they are outliers to all other Medusozoa in their surface area to volume relationships, deviating significantly from sphericity [37]. This suggests a different mechanism for their discharge that could be more reliant on capsule tension than on osmotic potentials [38], and strong selection for efficient nematocyst packing in the cnidoband [3,37]. Our results show that Codonophora underwent a shift towards elongation and Cystonectae towards sphericity, assuming the common ancestor had an intermediate state. Since we know that the haplonemes of other hydrozoan outgroups are generally spheroid, it is more parsimonious to assume that cystonects retain this ancestral state. Later, we observe a return to more rounded (ancestral) haplonemes in *Erenna*, concurrent with a secondary gain of a piscivorous trophic niche, like that exhibited by cystonects. [25] showed that haplonemes have a penetrating function as isorhizas in cystonects and an adhesive function as anisorrhizas in Tendiculophora. The two clades that have converged to feed primarily on fish (Cystonectae and Clade B, which includes *Erenna*, *Stephanomia*, *Marrus*, and rhodaliids) have also converged morphologically toward more compact haplonemes, significantly distinct from their closest relatives. Isorhizas in cystonects are known to penetrate the skin of fish during prey capture, and to deliver the toxins that aid in paralysis and digestion [39]. *Erenna*'s anisorrhizas are also able to penetrate human skin and deliver a painful sting [40] (and pers. obs.), a common feature of piscivorous cnidarians like the Portuguese man-o-war or box jellies.

The implications of these results for the evolution of nematocyst function are that an innovation in the discharge mechanism of haplonemes may have occurred during the main shift to elongation. Elongate nematocysts can be tightly packed into cnidobands. We hypothesize this may be a Tendiculophora lineage-specific adaptation to packing more nematocysts into a limited tentillum space, as suggested by [3]. [37] hypothesized that smaller, more spherical nematocysts, with a lower surface area to volume ratio, are more efficient in osmotic-driven discharge and thus have more power for skin penetration. The elongated haplonemes of

338 crustacean-eating Tendiculophora have never been observed penetrating their crustacean prey
339 ([25] and our unpublished observations), and are hypothesized to entangle the prey through
340 adhesion of the abundant spines to the exoskeletal surfaces and appendages. Entangling
341 requires less acceleration and power during discharge than penetration, as it does not rely
342 on point pressure. In fish-eating cystonects and *Erenna* species, the haplonemes are much
343 less elongated and very effective at penetration, in congruence with the osmotic discharge
344 hypothesis. Tendiculophora, comprised of the clades Euphysonectae and Calycophorae,
345 includes the majority of siphonophore species. Within these clades are the most abundant
346 siphonophore species, and a greater morphological and ecological diversity is found. We
347 hypothesize that this packing-efficient haploneme morphology may have been a key innovation
348 leading to the diversification of this clade. However, other characters that shifted concurrently
349 in the stem of this clade may have been responsible for their extant diversity.

350 *Phenotypic integration of siphonophore tentilla* – Our evolutionary rate covariance results
351 (SM36-38) indicate that tentilla are not only phenotypically integrated but also show patterns
352 of evolutionary modularity, where different sets of characters appear to evolve in stronger
353 correlations among each other than with other characters [41]. This may be indicative of the
354 underlying genetic and developmental dependencies among closely homologous nematocyst
355 types (such as desmonemes and rhopalonemes) and structures. In addition, these evolutionary
356 modules point to hypothetical functional modules. For example, the coiling degree of the
357 cnidoband and the extent of the involucrum have correlated rates of evolution, while high-
358 speed videos show that the involucrum helps direct the whiplash of the uncoiling cnidoband
359 distally (towards the prey).

360 While selection acting on character states is a widely studied phenomenon, recent studies
361 have shown that selection can also act upon the patterns of character correlations and
362 phenotypic dependencies [33,42–47]. This evolution of character relationships can allow
363 lineages to explore new regions of the morphospace and facilitate the appearance of ecological
364 novelties. Our results show that the patterns of phenotypic integration in siphonophore

365 tentilla vary among clades, and appear to display different relationships across shifting feeding
366 specializations. Similar to what has been found in the feeding morphologies of fish [33,48],
367 siphonophore tentilla may have accommodated new diets by altering the correlations between
368 characters. For example, changes in the size and shape relationships between nematocyst
369 types gave rise to the nematocyst complements specialized in ensnaring prey with different
370 combinations of defensive traits.

371 *Limitations* - While our results unambiguously show that tentillum morphology evolved
372 with diet, and strongly support deviations from the generalist-to-specialist evolution scenario,
373 the conclusions we can draw from these analyses are limited in several ways. The biggest
374 challenge at present is the sparse dietary data available in the literature. Additional dietary
375 data could reveal transitions from generalists to specialists we were unable to detect for
376 two reasons. First, some of the taxa in our dataset have a very limited number of feeding
377 observations, which could lead to apparent specialization. Second, some of the taxa not
378 included in our dataset could be undiscovered generalists. When interpreting these results, it
379 is also important to remember that diet is also dependent on environmental prey availability.
380 In addition, selectivity differences across siphonophore species could be also driven by other
381 phenotypes not accounted for in this study. Finally, further observations on behavior, digestion
382 biochemistry, and toxin composition are necessary to assess their relative importance in
383 determining diet.

384 Conclusions

385 Siphonophores occupy diverse predatory niches in the open ocean, ranging from mid-trophic
386 small-crustacean eaters to piscivorous super-carnivores. With the evolution of diversified
387 prey type specialization comes the evolution of morphologies adapted to the challenges posed
388 by different prey. The results presented here indicate that the associations found between
389 siphonophore tentilla and their prey are a product of correlated evolution in highly integrated
390 traits. While much of the feeding ecology literature focuses on how predatory generalists

391 evolve into predatory specialists, in siphonophores we find predatory specialists can evolve
392 into generalists, and that specialists on one prey type have directly evolved into specialists
393 on other prey types. We find that the character states, evolutionary optima, and genetic
394 correlations of many tentillum characters have evolved following these shifts in trophic niche.
395 Our extended morphological characterization shows that the relationships between form and
396 ecology hold across a large set of siphonophore taxa and characters, and can be used to
397 generate hypotheses on the feeding habits of uncharacterized species. We identify key aspects
398 of organismal trait evolution that are central to understanding the emergence of food web
399 complexity.

400 Materials and Methods

401 *Tentillum morphology* – The morphological work was carried out on siphonophore specimens
402 fixed in 4% formalin from the Yale Peabody Museum Invertebrate Zoology (YPM-IZ) collection
403 (accession numbers in Dryad repository). These specimens were collected intact across many
404 years of fieldwork expeditions, using blue-water diving [49], remotely operated vehicles (ROVs),
405 and human-operated submersibles. Tentacles were dissected from non-larval gastrozooids,
406 sequentially dehydrated into 100% ethanol, cleared in methyl salicylate, and mounted onto
407 slides with Canada Balsam or Permount mounting media. The slides were imaged as tiled
408 z-stacks using differential interference contrast (DIC) on an automated stage at YPM-IZ
409 (with the assistance of Daniel Drew and Eric Lazo-Wasem) and with laser point confocal
410 microscopy using a 488 nm Argon laser that excited autofluorescence in the tissues. Thirty
411 characters (defined in SM5) were measured using Fiji [50,51]. We did not measure the lengths
412 of contractile structures (terminal filaments, pedicles, gastrozooids, and tentacles) since they
413 are too variable to quantify. We measured at least one specimen for 96 different species
414 (raw data available in Dryad). Of these, we selected 38 focal species across clades based on
415 specimen availability and phylogenetic representation. Three to five tentacle specimens from
416 each one of these selected species were measured to capture intraspecific variation.

417 *Siphonophore phylogeny* – While the main goal of this work is not to elucidate a novel
418 phylogeny for Siphonophora, we did expand on the most recent transcriptome based phylogeny
419 [24] to accommodate a larger taxon sampling. In order to do this, we ran a constrained analysis
420 on an extensive 18S+16S dataset. The phylogenetic analysis included 55 siphonophore species
421 and 6 outgroup cnidarian species (*Clytia hemisphaerica*, *Hydra circumcincta*, *Ectopleura*
422 *dumortieri*, *Porpita porpita*, *Velella velella*, *Staurocladia wellingtoni*). The gene sequences we
423 used in this study are available online (accession numbers in Dryad repository). Some of the
424 sequences we used were accessioned in [27], and others we extracted from the transcriptomes
425 in [24]. Two new 16S sequences for *Frillagalma vityazi* (MK958598) and *Thermopalia* sp.
426 (MK958599) sequenced by Lynne Christianson using the primers from [52] (read 3' to 5'
427 F: TCGACTGTTACCAAAAAACATAGC , R: ACGGAATGAACTCAAATCATGTAAG)
428 were included and accessioned to NCBI. We aligned these sequences using MAFFT [53]
429 (alignments available in Dryad). We inferred a Maximum Likelihood (ML) phylogeny (SM6)
430 from 16S and 18S ribosomal rRNA genes using IQTree [54] with 1000 bootstrap replicates
431 (iqtree -s alignment.fa -nt AUTO -bb 1000). We used ModelFinder [55] implemented in
432 IQTree v1.5.5. to assess the relative model fit. ModelFinder selected GTR+R4 for having
433 the lowest Bayesian Information Criterion score. Additionally, we inferred a Bayesian tree
434 with each gene as an independent partition in RevBayes [56] (SM9 and SM11), which was
435 topologically congruent with the unconstrained ML tree. The *alpha* priors were selected to
436 minimize prior load in site variation.

437 Given the broader sequence sampling of the transcriptome phylogeny, we ran constrained
438 inferences (using both ML and Bayesian approaches, which produced fully congruent topologies
439 (SM8 and SM10)) after fixing the 5 nodes that were incongruent with the topology of the
440 consensus tree in [24]. This topology was then used to inform a Bayesian relaxed molecular
441 clock time-tree in RevBayes, using a birth-death process (sampling probability calculated
442 from the known number of described siphonophore species) to generate ultrametric branch
443 lengths (SM11-12). Scripts available in the Dryad repository.

Feeding ecology – We extracted categorical diet data for different siphonophore species from published sources, including seminal papers [4,25,57–61], and ROV observation data [22,62] with the assistance of Elizabeth Hetherington and C. Anela Choy (data available in Dryad repository). We removed the gelatinous prey observations for *Praya dubia* eating a ctenophore and a hydromedusa, and for *Nanomia* sp. eating *Aegina* since we believe these are rare events that have a much larger probability of being detected by ROV methods than their usual prey, and it is not clear whether the medusae were attempting to prey upon the siphonophores. Personal observations on feeding (from SHDH, CAC, and Philip Pugh) were also included for *Resomia ornicephala*, *Lychnagalma utricularia*, *Bargmannia amoena*, *Erenna richardi*, *Erenna laciniata*, *Erenna sirena*, and *Apolemia rubriversa*. In order to detect coarse-level patterns in feeding habits, the data were merged into feeding guilds. The feeding guilds described here are: small-crustacean specialist (feeding mainly on copepods and ostracods), large crustacean specialist (feeding on large decapods, mysids, or krill), fish specialist (feeding mainly on actinopterygian larvae, juveniles, or adults), gelatinous specialist (feeding mainly on other siphonophores, medusae, ctenophores, salps, and/or doliolids), and generalist (feeding on a combination of the aforementioned taxa, without favoring any one prey group). These were selected to minimize the number of categories while keeping the most different types of prey separate. We extracted copepod prey length data from [25]. To calculate specific prey selectivities, we extracted quantitative diet and zooplankton composition data from [58], matched each diet assessment to each prey field quantification by site, calculated Ivlev’s electivity indices [63], and averaged those by species (data available in the Dryad repository).

Statistical analyses – For subsequent comparative analyses, we removed species present in the tree but not represented in the morphology data, and *vice versa*. Although we measured specimens labeled as *Nanomia bijuga* and *Nanomia cara*, we are not confident in some of the species-level identifications, and some specimens were missing diagnostic zooids. Thus, we decided to collapse these into a single taxonomic concept (*Nanomia* sp.). All *Nanomia* sp.

471 observations were matched to the phylogenetic position of *Nanomia bijuga* in the tree. We
472 carried out all phylogenetic comparative statistical analyses in the programming environment
473 R [64], using the Bayesian ultrametric species tree (Fig. 2), and incorporating intraspecific
474 variation estimated from the specimen data as standard error whenever the analysis tool
475 allowed it. R scripts and summarized species-collapsed data available in the Dryad repository.
476 For each character (or character pair) analyzed, we removed species with missing data and
477 reported the number of taxa included. We tested each character for normality using the
478 Shapiro-Wilk test [65], and log-transformed those that were non-normal.

479 We fitted different models generating the observed data distribution given the phylogeny
480 for each continuous character using the function fitContinuous in the R package *geiger* [66].
481 We then ranked the models in order of increasing parametric complexity (WN, BM, EB,
482 OU), and compared the corrected Akaike Information Criterion (AICc) support scores [67]
483 to the lowest (best) score, using a cutoff of 2 units to determine significantly better support.
484 When the best fitting model was not significantly better than a less complex alternative, we
485 selected the least complex model (SM13). We calculated model adequacy scores using the
486 R package *arbutus* [68] (SM14). We calculated phylogenetic signal in each of the measured
487 characters using Blomberg's K [69] (SM13). We reconstructed ancestral states using ML (R
488 *phytools*::anc.ML [70]), and stochastic character mapping (R *phytools*::make.simmap) for
489 categorical characters. R scripts available in the Dryad repository.

490 In order to study the evolution of predatory specialization, we reconstructed components
491 of the diet and prey selectivity on the phylogeny using ML (R *phytools*::anc.ML). To identify
492 evolutionary associations of diet with tentillum and nematocyst characters, we compared the
493 performance of a neutral evolution model to that of a diet-driven directional selection model.
494 First, we collapsed the diet data into the five feeding guilds mentioned above (fish specialist,
495 small crustacean specialist, large crustacean specialist, gelatinous specialist, generalist), based
496 on which prey types they were observed consuming most frequently. Then, we reconstructed
497 the feeding guild ancestral states using the ML function ace (package *ape* [71]), removing tips

498 with no feeding data. The ML reconstruction was congruent with the consensus stochastic
499 character mapping (SM31). Then, using the package *OUwie* [72], we fitted an OU model with
500 multiple optima and rates of evolution matched to the reconstructed ancestral diet regimes,
501 a single optimum OU model, and a BM null model, inspired by the analyses in [73]. Finally,
502 we compared their AICc support values to select the best fitting model (SM15).

503 To model the evolutionary associations between individual tentillum and nematocyst
504 characters and the ability to capture particular prey types in the diet, we ran a series
505 of phylogenetic generalized linear models (R `phyloglm::phyloglm`) (SM21). In addition, we
506 ran a series of comparative analyses to address hypotheses of diet-tentillum relationships
507 posed in the literature. To test for correlated evolution among binary characters, we used
508 Pagel's test [74]. To characterize and evaluate the relationship between continuous characters,
509 we used phylogenetic generalized least squares regressions (PGLS) [75]. To compare the
510 evolution of continuous characters with categorical aspects of the diet, we carried out a
511 phylogenetic logistic regression (R `nlme::gls` using the 'corBrownian' function for the argument
512 'correlation').

513 In order to study correlations between the rates of evolution between different characters,
514 we fitted a set of evolutionary variance-covariance matrices [33] (R `phytools::evol.vcv`). When
515 fitting all covariance terms simultaneously (SM36-38), we selected the largest set of characters
516 that would allow the analysis to run without computational singularities. This excluded many
517 of the morphometric characters which are linearly dependent on other characters. Since the
518 functions do not tolerate missing data, we ran the analyses in two ways: One including all taxa
519 but transforming absent states to zeroes, and another removing the taxa with absent states.
520 To test whether phenotypic integration changes across selective regimes determined by the
521 reconstructed feeding guilds, we carried out character-pairwise variance-covariance analysis
522 comparing alternative models (R `phytools::evolvcv.lite`), including those where correlations
523 are the same across the whole tree and models where correlations differ between selective
524 regimes (SM42). These analyses could only be carried out on the subset of taxa for which diet

525 data is available, and only among character pairs that are not computationally singular for
526 that taxonomic subset. Finally, we compared regime-specific variance-covariance matrices to
527 the general matrix and to their preceding regime matrix to identify the changes in character
528 dependence unique to each regime (SM43). Gelatinous specialist correlations could only be
529 estimated for a small subset of characters present in *Apolemia* and should be interpreted
530 with care.

531 We carried out linear discriminant analysis of principal components (DAPC) using
532 the dapc function (R adegenet::dapc) [76]. This function allowed us to incorporate more
533 predictors than individuals. We generated discriminant functions for feeding guild, soft/hard-
534 bodied prey, and for the presence of copepods, fish, and shrimp (large crustaceans) in the
535 diet (SM16-20). From these DAPCs we obtained the highest contributing morphological
536 characters to the discrimination (characters in the top quartile of the weighted sum of the
537 linear discriminant loadings controlling for the eigenvalue of each discriminant). For each
538 DAPC we generated hypotheses about the diets of siphonophores outside the training set
539 (R adegenet::predict.dapc), incorporating prediction uncertainty as posterior probabilities
540 (SM16-20). In order to identify the sign of the relationship between the predictor characters
541 prey type presence in the diet, we then generated generalized logistic regression models (as
542 a type of generalized linear model, or GLM using R stats::glm) with the top contributing
543 characters (from the corresponding DAPC) as predictors. We also carried out these GLMs
544 on the Ivlev's selectivity indices for each prey type calculated from [58]. Additional details
545 on the optimization are available in the Supplementary Materials.

546 Supplementary Materials

547 Data available from the Dryad Digital Repository: <http://dx.doi.org/10.5061/dryad.NNNN>
548 Supplementary Materials are available in https://github.com/dunnlab/tentilla_morph/
549 Supplement_forShort.pdf

550 **Funding**

551 This work was supported by the Society of Systematic Biologists (Graduate Student Award
552 to A.D.S.); the Yale Institute of Biospheric Studies (Doctoral Pilot Grant to A.D.S.); and
553 the National Science Foundation (Waterman Award to C.W.D., and NSF-OCE 1829835 to
554 C.W.D., S.H.D.H., and C. Anela Choy). A.D.S. was supported by a Fulbright Spain Graduate
555 Studies Scholarship.

556 **Acknowledgements**

557 We wish to thank the crew and scientists of the R/V Western Flyer, who participated in
558 the collection of many of the specimens used in this study. We also want to thank Lynne
559 Christianson and Shannon Johnson from the Monterey Bay Aquarium Research Institute
560 for their assistance in the field as well as for sequencing some of the species included in this
561 phylogeny. In addition, we wish to thank Lourdes Rojas, Daniel Drew, and Eric Lazo-Wasem
562 for their assistance in imaging the fixed specimens and managing the collections. We thank
563 Dennis Pilarczyk for organizing the prey selectivity data, Michael Landis for helping design
564 the Bayesian analyses, and Joaquin Nunez for reviewing this manuscript. Furthermore, we
565 thank Elizabeth D. Hetherington and C. Anela Choy for collating the data on siphonophore
566 feeding and for reviewing the manuscript. Finally, we thank Philip Pugh, who confirmed
567 many of our specimen identifications and taught us valuable knowledge about siphonophores.

568 **References**

- 569 1. Schmitz O. Predator and prey functional traits: Understanding the adaptive machinery
570 driving predator–prey interactions. *F1000Research*. 2017;6.
- 571 2. Mapstone GM. Global diversity and review of siphonophorae (cnidaria: Hydrozoa).
572 *PLoS One*. 2014;9: e87737.
- 573 3. Skaer R. The formation of cnidocyte patterns in siphonophores. Academic Press New

- 574 York; 1988.
- 575 4. Mackie GO, Pugh PR, Purcell JE. Siphonophore Biology. *Advances in Marine Biology*.
- 576 1987;24: 97–262.
- 577 5. Purcell JE. Influence of siphonophore behavior upon their natural diets: Evidence for
- 578 aggressive mimicry. *Science*. 1980;209: 1045–1047.
- 579 6. Haddock SH, Dunn CW, Pugh PR, Schnitzler CE. Bioluminescent and red-fluorescent
- 580 lures in a deep-sea siphonophore. *Science*. 2005;309: 263–263.
- 581 7. Haddock SH, Dunn CW. Fluorescent proteins function as a prey attractant: Experi-
582 mental evidence from the hydromedusa *olindias formosus* and other marine organisms. *Biology*
- 583 open. 2015;4: 1094–1104.
- 584 8. Robison BH. Deep pelagic biology. *Journal of experimental marine biology and ecology*.
- 585 2004;300: 253–272.
- 586 9. Simpson GG. *Tempo and mode in evolution*. Columbia University Press; 1944.
- 587 10. Hardin G. The competitive exclusion principle. *science*. 1960;131: 1292–1297.
- 588 11. Hutchinson GE. The paradox of the plankton. *The American Naturalist*. 1961;95:
- 589 137–145.
- 590 12. Futuyma DJ, Moreno G. The evolution of ecological specialization. *Annual review of*
- 591 *Ecology and Systematics*. 1988;19: 207–233.
- 592 13. Siddall ME, Brooks DR, Desser SS. Phylogeny and the reversibility of parasitism.
- 593 *Evolution*. 1993;47: 308–313.
- 594 14. Hougen-Eitzman D, Rausher MD. Interactions between herbivorous insects and
- 595 plant-insect coevolution. *The American Naturalist*. 1994;143: 677–697.
- 596 15. Robinson BW, Wilson DS, Shea GO. Trade-offs of ecological specialization: An
- 597 intraspecific comparison of pumpkinseed sunfish phenotypes. *Ecology*. 1996;77: 170–178.
- 598 16. Kelley ST, Farrell BD. Is specialization a dead end? The phylogeny of host use in
- 599 *dendroctonus* bark beetles (scolytidae). *Evolution*. 1998;52: 1731–1743.
- 600 17. Stireman-III JO. The evolution of generalization? Parasitoid flies and the perils of

- 601 inferring host range evolution from phylogenies. *Journal of evolutionary biology*. 2005;18:
602 325–336.
- 603 18. Johnson KP, Malenke JR, Clayton DH. Competition promotes the evolution of host
604 generalists in obligate parasites. *Proceedings of the Royal Society B: Biological Sciences*.
605 2009;276: 3921–3926.
- 606 19. Nosil P. Transition rates between specialization and generalization in phytophagous
607 insects. *Evolution*. 2002;56: 1701–1706.
- 608 20. Hoberg EP, Brooks DR. A macroevolutionary mosaic: Episodic host-switching,
609 geographical colonization and diversification in complex host–parasite systems. *Journal of
610 Biogeography*. 2008;35: 1533–1550.
- 611 21. Hardy NB, Otto SP. Specialization and generalization in the diversification of
612 phytophagous insects: Tests of the musical chairs and oscillation hypotheses. *Proceedings of
613 the Royal Society B: Biological Sciences*. 2014;281: 20132960.
- 614 22. Choy CA, Haddock SH, Robison BH. Deep pelagic food web structure as revealed
615 by in situ feeding observations. *Proceedings of the Royal Society B: Biological Sciences*.
616 2017;284: 20172116.
- 617 23. Costello JH, Colin SP, Gemmell BJ, Dabiri JO, Sutherland KR. Multi-jet propulsion
618 organized by clonal development in a colonial siphonophore. *Nature communications*. 2015;6:
619 8158.
- 620 24. Munro C, Siebert S, Zapata F, Howison M, Serrano AD, Church SH, et al. Improved
621 phylogenetic resolution within siphonophora (cnidaria) with implications for trait evolution.
622 *Molecular Phylogenetics and Evolution*. 2018.
- 623 25. Purcell JE. The functions of nematocysts in prey capture by epipelagic siphonophores
624 (coelenterata, hydrozoa). *The Biological Bulletin*. 1984;166: 310–327.
- 625 26. Purcell J, Mills C. The correlation of nematocyst types to diets in pelagic hydrozoa.
626 In “the biology of nematocysts”.(Eds da hessinger and hm lenhoff.) pp. 463–485. Academic
627 Press: San Diego, CA; 1988.

- 628 27. Dunn CW, Pugh PR, Haddock SH. Molecular phylogenetics of the siphonophora
629 (cnidaria), with implications for the evolution of functional specialization. *Systematic biology*.
630 2005;54: 916–935.
- 631 28. Nosil P, Mooers A. Testing hypotheses about ecological specialization using phyloge-
632 netic trees. *Evolution*. 2005;59: 2256–2263.
- 633 29. Martins EP. Phylogenies, spatial autoregression, and the comparative method: A
634 computer simulation test. *Evolution*. 1996;50: 1750–1765.
- 635 30. Harmon LJ, Losos JB, Jonathan Davies T, Gillespie RG, Gittleman JL, Bryan
636 Jennings W, et al. Early bursts of body size and shape evolution are rare in comparative
637 data. *Evolution: International Journal of Organic Evolution*. 2010;64: 2385–2396.
- 638 31. Uhlenbeck GE, Ornstein LS. On the theory of the brownian motion. *Physical review*.
639 1930;36: 823.
- 640 32. Butler MA, King AA. Phylogenetic comparative analysis: A modeling approach for
641 adaptive evolution. *The American Naturalist*. 2004;164: 683–695.
- 642 33. Revell LJ, Collar DC. Phylogenetic analysis of the evolutionary correlation using
643 likelihood. *Evolution: International Journal of Organic Evolution*. 2009;63: 1090–1100.
- 644 34. Longhurst AR. The structure and evolution of plankton communities. *Progress in
645 Oceanography*. 1985;15: 1–35.
- 646 35. O'Brien TD. COPEPOD, a global plankton database: A review of the 2007 database
647 contents and new quality control methodology. 2007.
- 648 36. Kayal E, Bentlage B, Cartwright P, Yanagihara AA, Lindsay DJ, Hopcroft RR, et al.
649 Phylogenetic analysis of higher-level relationships within hydroidolina (cnidaria: Hydrozoa)
650 using mitochondrial genome data and insight into their mitochondrial transcription. *PeerJ*.
651 2015;3: e1403.
- 652 37. Thomason J. The allometry of nematocysts. *The biology of nematocysts*. Elsevier;
653 1988. pp. 575–588.
- 654 38. Carré D, Carré C. On triggering and control of cnidocyst discharge. *Marine &*

- 655 Freshwater Behaviour & Phy. 1980;7: 109–117.
- 656 39. Hessinger DA. Nematocyst venoms and toxins. The biology of nematocysts. Elsevier;
- 657 1988. pp. 333–368.
- 658 40. Pugh P. A review of the genus *erenna bedot*, 1904 (siphonophora, physonectae).
- 659 BULLETIN-NATURAL HISTORY MUSEUM ZOOLOGY SERIES. 2001;67: 169–182.
- 660 41. Wagner GP. Homologues, natural kinds and the evolution of modularity. American
- 661 Zoologist. 1996;36: 36–43.
- 662 42. Young NM, HallgrÍmsson B. Serial homology and the evolution of mammalian limb
- 663 covariation structure. Evolution. 2005;59: 2691–2704.
- 664 43. Goswami A. Morphological integration in the carnivoran skull. Evolution. 2006;60:
- 665 169–183.
- 666 44. Monteiro LR, Nogueira MR. Adaptive radiations, ecological specialization, and the
- 667 evolutionary integration of complex morphological structures. Evolution: International
- 668 Journal of Organic Evolution. 2010;64: 724–744.
- 669 45. Hallgri'msson B, Jamniczky HA, Young NM, Rolian C, SCHMIDT-OTT U, Marcucio
- 670 RS. The generation of variation and the developmental basis for evolutionary novelty. Journal
- 671 of Experimental Zoology Part B: Molecular and Developmental Evolution. 2012;318: 501–517.
- 672 46. Claverie T, Patek S. Modularity and rates of evolutionary change in a power-amplified
- 673 prey capture system. Evolution. 2013;67: 3191–3207.
- 674 47. Caetano DS, Harmon LJ. Estimating correlated rates of trait evolution with uncertainty.
- 675 Systematic biology. 2018;68: 412–429.
- 676 48. Collar DC, Near TJ, Wainwright PC. Comparative analysis of morphological diversity:
- 677 Does disparity accumulate at the same rate in two lineages of centrarchid fishes? Evolution.
- 678 2005;59: 1783–1794.
- 679 49. Haddock SH, Heine JN. Scientific blue-water diving. California Sea Grant College
- 680 Program; 2005.
- 681 50. Collins TJ. ImageJ for microscopy. Biotechniques. 2007;43: S25–S30.

- 682 51. Schindelin J, Arganda-Carreras I, Frise E, Kaynig V, Longair M, Pietzsch T, et al.
- 683 Fiji: An open-source platform for biological-image analysis. *Nature methods*. 2012;9: 676.
- 684 52. Cunningham CW, Buss LW. Molecular evidence for multiple episodes of paedo-
- 685 morphosis in the family hydractiniidae. *Biochemical Systematics and Ecology*. 1993;21:
- 686 57–69.
- 687 53. Katoh K, Misawa K, Kuma K-i, Miyata T. MAFFT: A novel method for rapid
- 688 multiple sequence alignment based on fast fourier transform. *Nucleic acids research*. 2002;30:
- 689 3059–3066.
- 690 54. Nguyen L-T, Schmidt HA, Haeseler A von, Minh BQ. IQ-tree: A fast and effective
- 691 stochastic algorithm for estimating maximum-likelihood phylogenies. *Molecular biology and*
- 692 *evolution*. 2014;32: 268–274.
- 693 55. Kalyaanamoorthy S, Minh BQ, Wong TK, Haeseler A von, Jermiin LS. ModelFinder:
- 694 Fast model selection for accurate phylogenetic estimates. *Nature methods*. 2017;14: 587.
- 695 56. Höhna S, Landis MJ, Heath TA, Boussau B, Lartillot N, Moore BR, et al. RevBayes:
- 696 Bayesian phylogenetic inference using graphical models and an interactive model-specification
- 697 language. *Systematic Biology*. 2016;65: 726–736.
- 698 57. Biggs DC. Field studies of fishing, feeding, and digestion in siphonophores. *Marine &*
- 699 *Freshwater Behaviour & Phy*. 1977;4: 261–274.
- 700 58. Purcell J. Dietary composition and diel feeding patterns of epipelagic siphonophores.
- 701 *Marine Biology*. 1981;65: 83–90.
- 702 59. Pugh P, Youngbluth M. Two new species of prayine siphonophore (calycophorae,
- 703 prayidae) collected by the submersibles johnson-sea-link i and ii. *Journal of Plankton Research*.
- 704 1988;10: 637–657.
- 705 60. Bardi J, Marques AC. Taxonomic redescription of the portuguese man-of-war, physalia
- 706 physalis (cnidaria, hydrozoa, siphonophorae, cystonectae) from brazil. *Iheringia Série Zoologia*.
- 707 2007;97: 425–433.
- 708 61. Andersen OGN. Redescription of marrus orthocanna (kramp, 1942)(Cnidaria,

- 709 siphonophora). Zoological Museum, University of Copenhagen; 1981.
- 710 62. Hissmann K. In situ observations on benthic siphonophores (physonectae: Rhodaliidae)
711 and descriptions of three new species from indonesia and south africa. Systematics and
712 Biodiversity. 2005;2: 223–249.
- 713 63. Jacobs J. Quantitative measurement of food selection. Oecologia. 1974;14: 413–417.
- 714 64. Team RC. R: A language and environment for statistical computing. Vienna, austria:
715 R foundation for statistical computing; 2017. ISBN3-900051-07-0 <https://www.R-project.org>.
716 org; 2017.
- 717 65. Shapiro SS, Wilk MB. An analysis of variance test for normality (complete samples).
718 Biometrika. 1965;52: 591–611.
- 719 66. Harmon LJ, Weir JT, Brock CD, Glor RE, Challenger W. GEIGER: Investigating
720 evolutionary radiations. Bioinformatics. 2007;24: 129–131.
- 721 67. Sugiura N. Further analysts of the data by akaike's information criterion and the finite
722 corrections: Further analysts of the data by akaike's. Communications in Statistics-Theory
723 and Methods. 1978;7: 13–26.
- 724 68. Pennell MW, FitzJohn RG, Cornwell WK, Harmon LJ. Model adequacy and the
725 macroevolution of angiosperm functional traits. The American Naturalist. 2015;186: E33–
726 E50.
- 727 69. Blomberg SP, Garland T, Ives AR. Testing for phylogenetic signal in comparative
728 data: Behavioral traits are more labile. Evolution. 2003;57: 717–745.
- 729 70. Revell LJ. Phytools: An r package for phylogenetic comparative biology (and other
730 things). Methods in Ecology and Evolution. 2012;3: 217–223.
- 731 71. Paradis E, Blomberg S, Bolker B, Brown J, Claude J, Cuong HS, et al. Package “ape”.
732 Analyses of phylogenetics and evolution, version. 2019; 2–4.
- 733 72. Beaulieu J, O'Meara B. OUwie: Analysis of evolutionary rates in an ou framework.
734 R package version 1.17. 2012.
- 735 73. Cressler CE, Butler MA, King AA. Detecting adaptive evolution in phylogenetic

⁷³⁶ comparative analysis using the ornstein–uhlenbeck model. *Systematic biology*. 2015;64:
⁷³⁷ 953–968.

⁷³⁸ 74. Pagel M. Detecting correlated evolution on phylogenies: A general method for the
⁷³⁹ comparative analysis of discrete characters. *Proceedings of the Royal Society of London*
⁷⁴⁰ Series B: Biological Sciences. 1994;255: 37–45.

⁷⁴¹ 75. Grafen A. The phylogenetic regression. *Philosophical Transactions of the Royal*
⁷⁴² Society of London B, Biological Sciences. 1989;326: 119–157.

⁷⁴³ 76. Jombart T, Devillard S, Balloux F. Discriminant analysis of principal components: A
⁷⁴⁴ new method for the analysis of genetically structured populations. *BMC genetics*. 2010;11:
⁷⁴⁵ 94.